Presented at the International Workshop on Collective Effects and Impedance for B-Factoruies, KEK, Tsukuba, Japan, June 1995

The Interaction between a Beam and a Superconducting Cavity Module: Measurements in CESR and CESR-Phase III Goals*

S. Belomestnykh†, G. Flynn‡, W. Hartung, J. Kirchgessner, D. Moffat, H. Muller, H. Padamsee, M. Pisharody, and V. Veshcherevich†
Laboratory of Nuclear Studies, Cornell University, Ithaca, NY 14853 USA

INTRODUCTION

Plans for the next generation of electron-positron colliders (B-factories and B-factory-like machines) call for high beam currents to produce luminosities of the order of 10^{33}. To store these high currents in a machine, special attention must be paid to the interaction of the beam with discontinuities in the surrounding vacuum chamber. RF cavities are among the biggest perturbations in accelerator vacuum chambers and are therefore among the biggest sources of beam instabilities. Accelerating structures for new machines are being designed to have smaller impedance to reduce the beam-cavity interaction. Several new designs for both normal and superconducting cavities are now being considered at various laboratories [1].

The phased luminosity upgrade program for CESR calls for a total current of 1A in two beams [2]. The existing normal conducting copper cavities are to be replaced with superconducting niobium cavities. Quality factors of less than 100 are required for the dangerous cavity higher-order modes (HOMs) [3, 4].

Figure 1 shows a schematic of the entire module which includes the cavity, a 24 cm round beam pipe, a fluted beam pipe, two ferrite HOM loads, sliding joints, gate valves, and tapers to the CESR beam pipe.

The beam tubes were designed so that all of the HOMs propagate out of the cavity and are damped by the ferrite HOM loads, which are located outside the cryostat and which are an integral part of the beam tube.

Prototypes for the cavity, input coupler, cryostat, and HOM loads were subjected to a beam test in CESR in August 1994. Figures 2 - 4 show photographs of the HOM load, cavity, and cryostat being installed in CESR. A superconducting (SRF) cavity was installed in addition to the four five-cell normal conducting (NRF) cavities. The results of the test have been reported at the PAC'95 conference [5-7]. In this paper we review the results from the perspective of the CESR Phase III upgrade plan.

SYSTEM PERFORMANCE

The performance of the SRF system as a whole and cavity in particular was quite good. Below we briefly review some important results achieved in the beam test.

---

* Work supported by National Science Foundation, with supplementary support from the US-Japan Collaboration.

† Visitor from Budker Institute of Nuclear Physics, 630090 Novosibirsk, Russia

‡ Visitor from LURE, 91405 Orsay, France

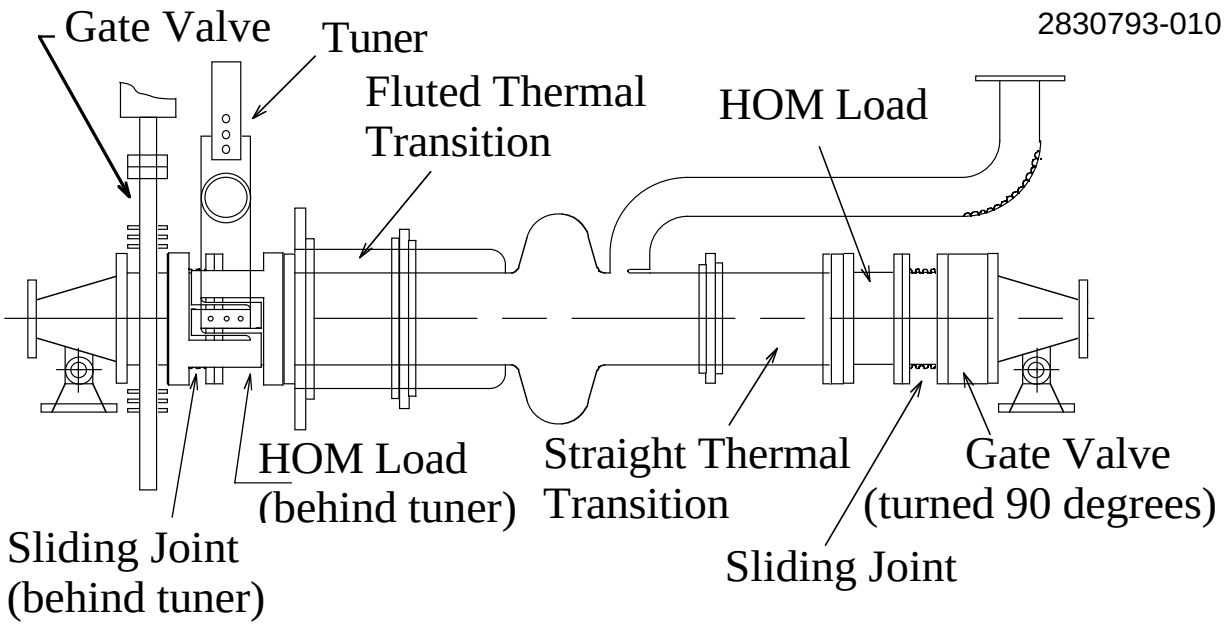

Figure 1. Schematic of the SRF cavity module.

Accelerating Gradients

Before the beam test, the niobium cavity was tested in a vertical cryostat up to an accelerating gradient of 10 MV/m [8]. The cavity was then tested in its horizontal cryostat with high RF power (without beam). After processing to 6 MV/m CW, it was installed in CESR.

Throughout most of the test, we kept the accelerating gradient of the cavity at 4.5 MV/m. A special run was dedicated to investigation of the behavior of our system at higher gradients. At 5 MV/m, the cavity was run stably for 1/2 hour with 100 - 110 mA beam current.

The cavity could only be operated for short periods above 5 MV/m, because of increased dissipation due to field emission, which caused the cryostat pressure to increase steadily. The pressure increase required tuner motion to maintain the correct cavity frequency; eventually the tuner ran into its safety stop. Nevertheless, we were able to run the cavity for few minutes with beam currents between 95 and 120 mA and a cavity gradient of up to 6 MV/m. A gradient of 6 MV/m is our goal for Phase III.

Beam Current

The maximum current for the test was 220 mA (in 27 bunches, distributed into 9 trains of 3 bunches with $1.3 \cdot 10^{11}$ particles per bunch). The current limit was set not by the performance of the cavity but by the heating of other CESR components. The maximum single-bunch current was 44 mA ($7 \cdot 10^{11}$ particles), with the limit again set by heating of other CESR components. Note that the product of the number of bunches times the square of the single bunch current was nearly the same as for the 220 mA, 27 bunch case. We are a factor of 6 below the CESR-Phase III goal, which calls for a beam current of 500 mA in 45 bunches (9 trains of 5 bunches) for each beam.

RF Power

A special experiment was dedicated to delivering the maximum RF power to the beam. The relative phase between the NRF and SRF cavities was adjusted so that the bunches went through the SRF cavity at the peak of the SRF voltage. The NRF cavities provided longitudinal

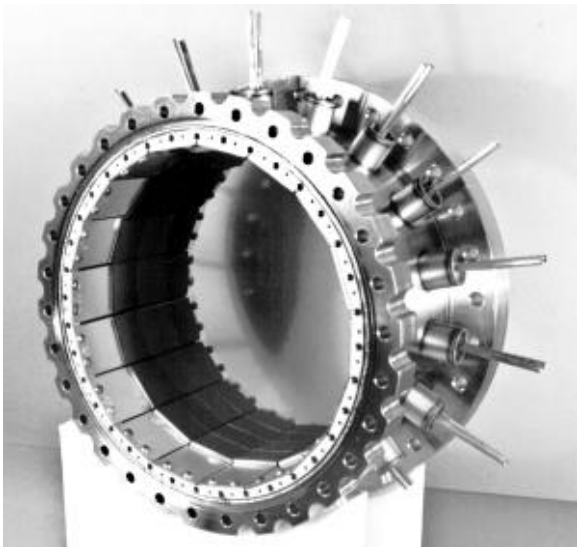

Figure 2. “Porcupine” HOM load near the end of construction.

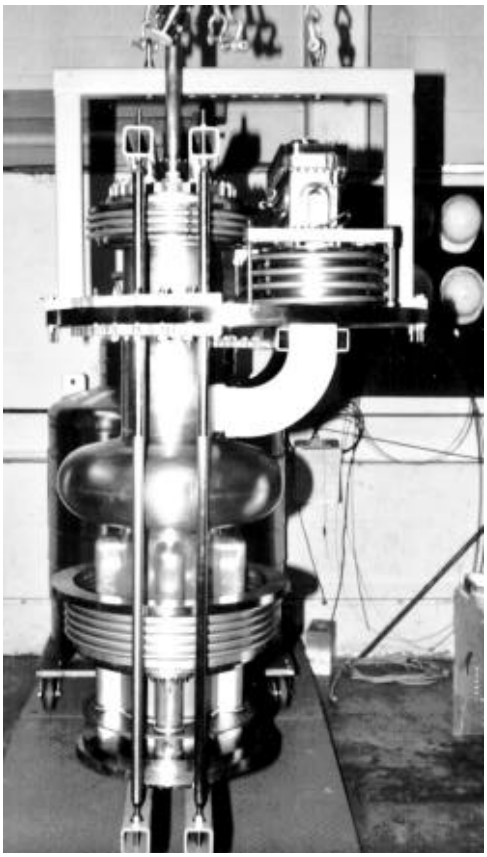

Figure 3. Niobium cavity being prepared for assembly into horizontal cryostat.

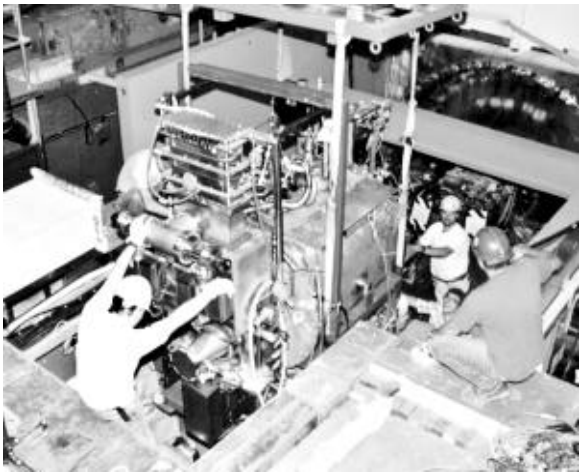

Figure 4. Cryostat being installed in CESR.

beam stability and extracted the excess power delivered to the beam from the SRF cavity.

The maximum power delivered to the beam by the SRF cavity was 155 kW, a factor of 2 above the world record set by the SRF cavity tested in TRISTAN-AR at 2 MV/m [9], but still a factor of 2 less than the Phase III goal. Vacuum bursts and arc trips near the RF window prevented us from going higher. We hope that new planar waveguide RF window, recently tested at LNS [10], will allow us to reach the Phase III requirement.

BEAM-CAVITY INTERACTION MEASUREMENTS

Studies of the beam-cavity interaction were conducted with a variety of bunch configurations: single bunch, 9 bunches per beam, and 9 trains of 2 or 3 bunches per train. We used a high energy lattice for most of the experiments; a low energy lattice was also used to

Table 1. Selected Parameters of the CESR Storage Ring

Parameter	High Energy Lattice	Low Energy Lattice
Ring circumference	768.4 m	
Revolution frequency	390.15 kHz	
RF Frequency	499.78 MHz	
Beam energy	5.265 GeV	4.400 GeV
SR energy loss per turn	1.0105 MeV	0.4928 MeV
Momentum compaction	0.01142	0.00926
RMS energy spread	$6.122 \cdot 10^{-4}$	$5.116 \cdot 10^{-4}$

measure the loss factor vs. bunch length. Some machine parameters for these optics are given in Table 1.

Power Dissipated in the HOM Loads and Loss Factor

We measured the temperature of the input and output cooling water for each HOM load, along with the water flow rate. The values yield the power transferred to the water from the ferrite:

$$P = \sum_{i=1}^{2} v_f^i \, C \, \rho \, (T_{out}^i - T_{in}^i) \, ,$$

where P is the power transferred to the cooling water from the two HOM loads; v_f is the water flow rate; C is the specific heat capacity of the water; ρ is the water density; T_{out} and T_{in} are the output and input temperatures of the cooling water.

This power should be approximately equal to the power lost by the beam due to its interaction with the cavity structure below the cutoff frequencies of the beam pipes because (i) in our HOM load design [6], other heat transfer mechanisms (conduction through the copper plate to the stainless steel shell, and heat radiation) should not give a significant contribution relative to the water cooling, and (ii) the HOMs with resonant frequencies below the cutoff frequencies of the nearby beam pipes (2.2 GHz and 3.4 GHz) are trapped inside the accelerating structure, so all their energy should be dissipated in the lossy material of the HOM loads.

We used the two lattices to obtain bunch lengths between 10 and 25 mm. Uniformly-filled bunches were used. Most measurements were done with one or 9 bunches. For uniformly-filled bunches, the loss factor is given by

$$k = \frac{N P f_{rev}}{I_o^2} \, ,$$

where I_o is the average beam current; f_{rev} is the revolution frequency; N is the number of bunches.

We do not have a bunch length monitor for CESR, but previous measurements [11, 12] indicate that there is no bunch lengthening in the storage ring; so we can calculate the bunch length via

$$\sigma_l = \frac{\alpha \, c}{\Omega_s} \cdot \frac{\sigma_E}{E_o} \, ,$$

$$\Omega_s^2 = \omega_{rev}^2 \cdot \frac{\alpha \, h \, e \sqrt{V_{RF}^2 - (U_o/e + U_{coh}/e)^2}}{2\pi E_o} \, ,$$

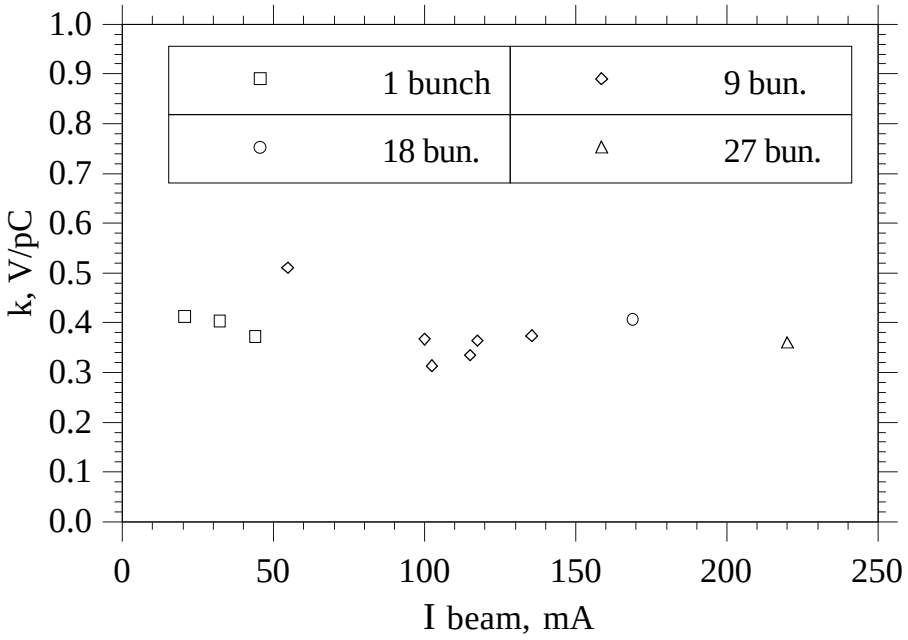

Figure 5. The loss factor of the SRF cavity vs. total beam current.

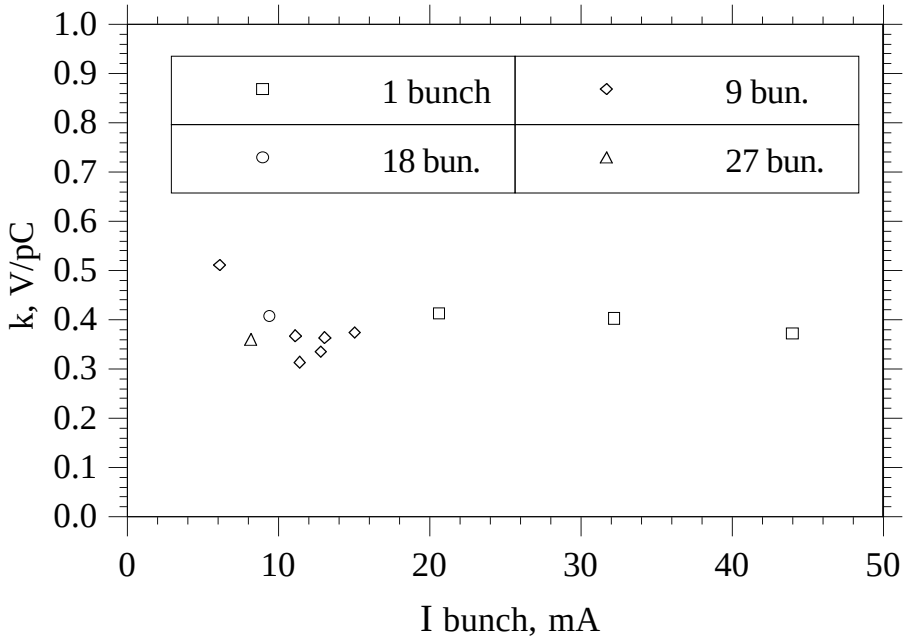

Figure 6. The loss factor of the SRF cavity vs. current per bunch.

where α is the momentum compaction factor; c is the speed of light; Ω_s is the synchrotron frequency; σ_E is the energy spread; h is the RF harmonic number, E_o is the beam energy; V_{RF} is the RF voltage; U_o is the energy loss per turn due to synchrotron radiation; and U_{coh} is the coherent energy loss per turn due to the total loss factor of the ring.

To verify that we do not have bunch lengthening, the loss factor was plotted as function of beam current for the same machine optics (high energy lattice) and RF voltage (Figures 5 and 6).

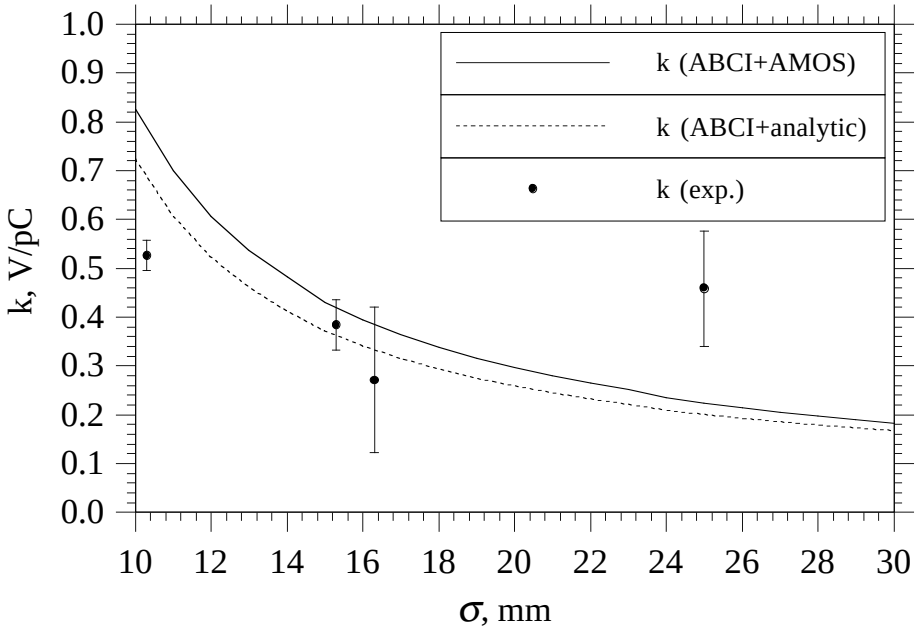

Figure 7. The loss factor of the SRF cavity assembly (experimental data and prediction).

The theoretical bunch length σ_l is equal to 15.3 mm for these measurements. One can see that the loss factor does not depend on current, i.e. there is no evidence of bunch lengthening.

The experimental results for the loss factor versus bunch length are compared with the predictions [6] in Figure 7. One can see that there is some disagreement for the shortest bunch length. That disagreement may be due to propagation of some portion of the HOM power into the beam pipes for frequencies above cutoff. There is also a big disagreement for the 25 mm bunch length. That data point was obtained with the low-energy lattice, using only the SRF voltage (with the NRF system switched off and the NRF cavities detuned). Unfortunately, the accelerating voltage was not high enough to allow us make measurements with high beam current: the total current was limited to 29 mA in 9 bunches due to the poor life time. The signal was therefore small, and this data point may have a big systematic error.

The maximum HOM power extracted by the two HOM loads was 2 kW, which is about 10 times less than needed for CESR-III. In a separate high power test of an HOM load, however, we reached a dissipated power of 14 kW (per load) [6] which is higher than the Phase III goal.

Sampling the Wake Potential with Two Bunches

An elegant method of the wake potential sampling, proposed recently by A. Temnykh [13], was used in the beam test: with two bunches of equal current, placed close to each other, we can measure the power loss due to some impedance. By varying the distance between the bunches, we can obtain information about the time structure of the wake potential. Also, we can calculate the loss factor and wake potentials for the two-bunch case using computer codes like ABCI [14] and AMOS [15] and compare these calculations with the measured values.

Using the definition of loss factor given above, we see that the loss factor for two bunches will be equal to the loss factor of a single bunch if the wake potential decays completely before the arrival of the second bunch, or if the HOMs with high *R/Q*s are all detuned far enough from harmonics of one half the RF frequency (so that the wake fields are not close to being completely in phase or completely out of phase).

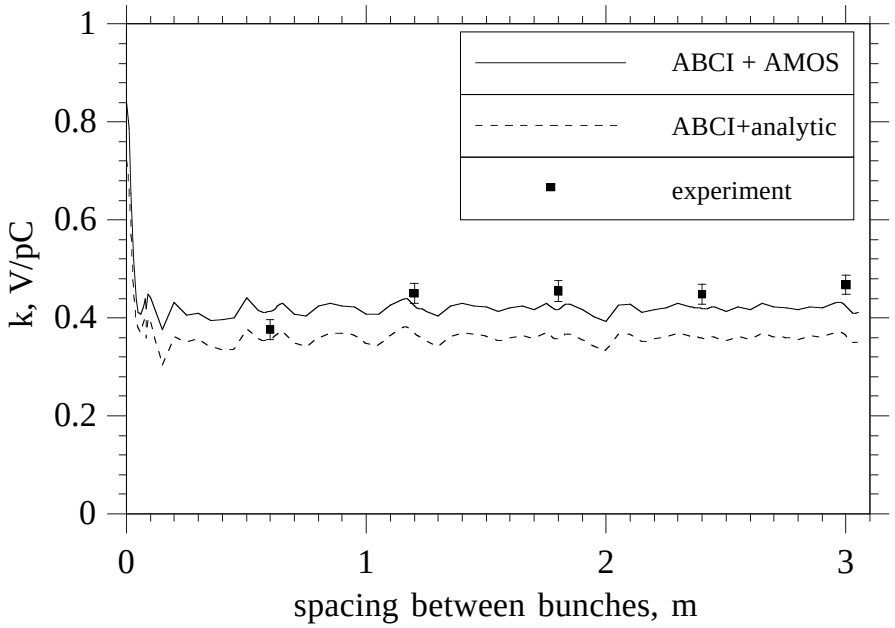

Figure 8. The loss factor of the SRF cavity assembly sampled by two bunches (experimental data and prediction).

The minimum spacing between two bunches is equal to the wavelength of the RF system, i.e. 60 cm for CESR. We measured the power dissipation in the HOM loads of the cavity module calorimetrically and varied the bunch spacing from 1 to 5 buckets. The measurements were done with a beam energy of 5.3 GeV and three different total beam currents: 10, 20, and 30 mA. Figure 8 shows the measured loss factor in comparison with ABCI and AMOS calculations. The agreement is very good.

Total Loss Factor of the Ring

Higher mode losses in CESR have been studied by M. Billing [16]. Scaling laws for the loss factor of different components in the vacuum chamber are in good agreement with experimental data; we used them to predict the total loss factor of the machine under the conditions of our test. Both the predictions and the separate calorimetric measurements of the loss factor of the superconducting cavity module show that the loss factor of the SRF cavity is much less than the total CESR loss factor. Nevertheless we measured the total loss factor of the machine before and after installation of the SRF cavity, to make sure that there were no gross errors in the calorimetric measurements. The predicted and measured total CESR loss factors are shown in the Fig. 9.

Dipole Loss Factor

We tried to measure the dipole component of the cavity loss factor by displacing a 120 mA (in 9 bunches) beam (with a bunch length of about 15 mm) horizontally and vertically by ±10 mm in the SRF cavity. According to calculations, the monopole component of the loss factor is 0.43 V/pC, and the dipole component is 0.006 V/pC for a 10 mm beam displacement. The cooling water ΔT was about 3.5°C for each HOM load. That means that the contribution from the dipole component should be of order 0.05°C. The resolution of our calorimetry is 0.03°C, and the noise level is of the same order. No changes in the cooling water ΔT were seen in excess of the resolution and noise level of the measurement.

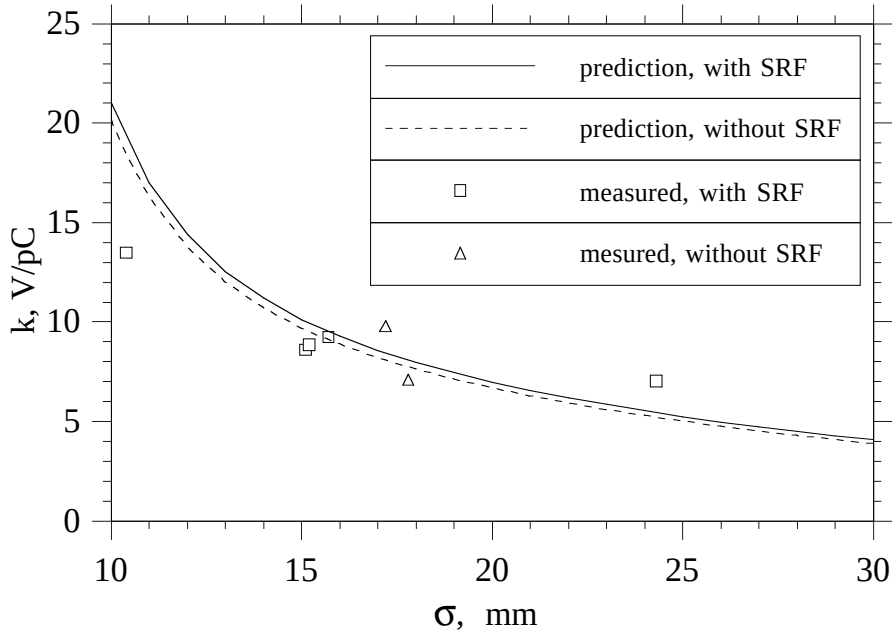

Figure 9. The total CESR loss factor (experimental data and prediction).

Sweeping HOM Frequencies with the Tuner and HOM Spectra

Using the cavity's fundamental mode frequency tuner, we changed the HOM frequencies to investigate the influence of the HOMs on the beam dynamics and to look for any unexpectedly dangerous (high $R/Q * Q$) HOMs. In these tests, the RF power for the SRF cavity was switched off and the fundamental mode frequency remained detuned. While scanning the tuner position, we were able to maintain a 100 mA beam, and there were no beam instabilities. We continuously monitored the HOM power deposited by the beam. The loss factor was calculated from the power dissipation in the HOM loads. The dependence of the loss factor on tuner position is shown in Figure 10. The small variation of the loss factor shows that there was no resonant excitation of HOMs as their frequencies changed. In addition, we measured the tunes and damping times of coupled bunch modes with a nine bunch beam, using a spectrum analyzer, for two positions of the tuner. The technique of these measurements is the same as described in [17]. No significant changes in damping times or tunes were observed between the two tuner positions: all changes were within the repeatability of the measurements.

We searched for dangerous HOMs by exciting the cavity via a single-bunch beam of 30 mA and varying the transverse displacement of the beam. The HOM spectra were observed and recorded using a spectrum analyzer.

We used results from URMEL [18] and CLANS [19] (for monopole HOMs) calculations [20] and measurements on a copper model of the cavity [21] to compare with the beam test measurements. Unfortunately we were not very successful in our attempts to match up the HOMs, though we can say that, for monopole HOMs, Q-factors are of order of 100, and for dipole and quadrupole HOMs, Q-factors are typically less than 1000. This is consistent with previous measurements. No resonant excitation of HOMs or beam instabilities were observed.

Synchrotron Radiation Heating

The position of the SRF cavity in CESR was such that dipole magnets were located < 1 m away from one side; on the other side, the closest magnet was >15 m away. Most of the tests were carried out with a positron beam, so as not to irradiate the cavity region with an excessive

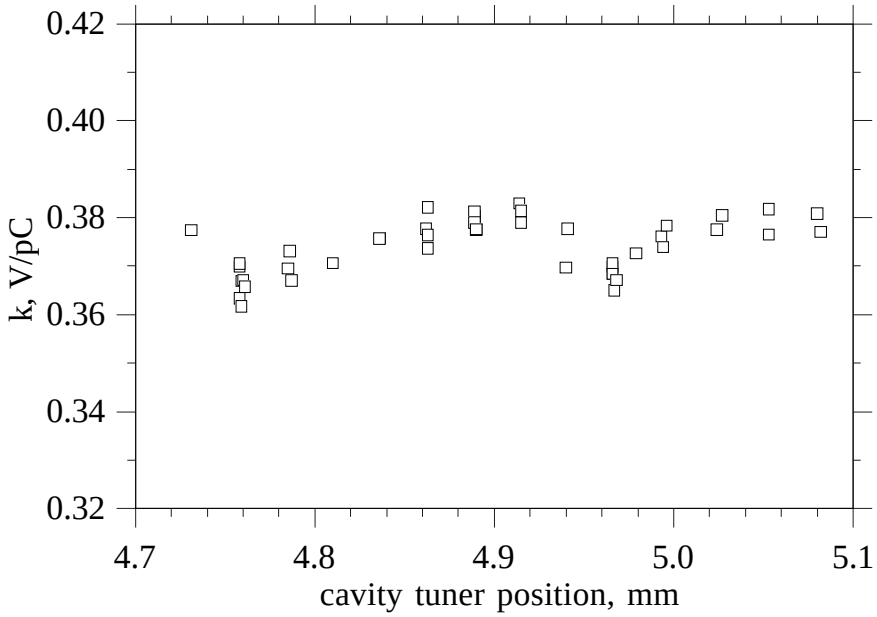

Figure 10. Dependence of the cavity loss factor on the cavity tuner position.

dose of synchrotron radiation (SR) from the nearby bending magnet. Near the end of the test, however, a 57 mA electron beam (in 9 bunches) was also run through the cavity, to see how the cavity performed in the presence of a severe SR dose. With 100 W of synchrotron radiation power incident on the stainless steel taper, its temperature increased to 100^{o}C and the vacuum degraded from $6{\cdot}10^{-9}$ to $6{\cdot}10^{-8}$ torr. The cavity operated stably in the presence of this large SR dose and there was no increase in cryogenic losses. In order to reduce the temperature rise and vacuum degradation, we plan to add water cooling and SR masks to the tapers.

CONCLUSIONS

The calorimetry and RF power results agree with predictions up to their respective uncertainties. The results of wake potential sampling suggest that the wake fields of the SRF cavity will not limit the performance of CESR in bunch train operation. No beam instabilities or dangerous HOMs were encountered while sweeping the HOM frequencies using the cavity tuner or while exciting multipole HOMs by displacing the beam off axis.

The next step in the RF system upgrade for CESR-III will be to replace one of the NRF cavities with an SRF cavity in a new cryostat for a long-term test, which is scheduled to begin in late summer of 1996.

ACKNOWLEDGEMENTS

We would like to thank our colleagues P. Barnes and J. Sears for valuable assistance in many stages of the preparations for the beam test as well as during beam test itself; R. Ehrlich and E. Nordberg, who were responsible for the refrigerator and cryogenic distribution system; R. Kaplan and J. Reilly for their extremely useful help with the RF system operation. Our special

thanks to Prof. D. Rubin, Prof. M. Tigner, M. Billing, and D. Rice for their help and guidance throughout the beam test. We appreciate S. Peck's design of a special low energy lattice for the beam test. Also, we are pleased to thank S. Henderson for calculation of SR power and B. Vakoc for help with numerous computer calculations. We acknowledge the valuable contribution of E. Chojnacki during the test of the new RF window. Finally, we wish to thank all of the Laboratory staff, and the CESR operations staff in particular, who helped to make the beam test possible.

REFERENCES

[1] J. Kirchgessner, "Review of the Development of RF Cavities for High Currents", *presented at the 1995 Particle Accelerator Conference, Dallas, TX* (to be published)

[2] D. Rubin, "CESR Status and Plans", *presented at the 1995 Particle Accelerator Conference, Dallas, TX* (to be published)

[3] H. Padamsee, et al., "Accelerating Cavity Development for the Cornell B-Factory, CESR-B", *Conference Record of the 1991 Particle Accelerator Conference,* Vol. 2, pp. 786-788, San Francisco, CA, May 1991

[4] H. Padamsee, et al., "Design Challenges for High Current Storage Rings", *Particle Accelerators,* 1992, Vol. 40, pp. 17-41

[5] H. Padamsee, et al., "Beam Test of a Superconducting Cavity for the CESR Luminosity Upgrade", *presented at the 1995 Particle Accelerator Conference, Dallas, TX* (to be published)

[6] S. Belomestnykh, et al., "Comparison of the Predicted and Measured Loss Factor of the Superconducting Cavity Assembly for the CESR Upgrade", *presented at the 1995 Particle Accelerator Conference, Dallas, TX* (to be published), also *Cornell LNS Report SRF 950406-04* (1995)

[7] S. Belomestnykh et al., "Wake fields and HOMs Studies of a Superconducting Cavity Module with the CESR Beam", *presented at the 1995 Particle Accelerator Conference, Dallas, TX* (to be published)

[8] D. Moffat, et al., "Preparation and Testing of a Superconducting Cavity for CESR-B", *Proceedings of the 1993 Particle Accelerator Conference,* Vol. 2, pp. 763-765, Washington, D.C., May 1993

[9] K. Akai, et al., "Beam Tests and Operation of Superconducting Cavities", *Proceedings of the 4th Workshop on RF Superconductivity,* KEK Report 89-21, Vol. 1, pp. 189-206, KEK, Tsukuba, Japan, August 1989

[10] M. Pisharody, et al., "Planar Waveguide Window for the CESR Upgrade", *presented at the 1995 Particle Accelerator Conference, Dallas, TX* (to be published)

[11] E. B. Blum, et al., "Bunch Length Measurements in CESR Using an X-Ray Sensitive Photoconducting Detector", *Nuclear Instruments and Methods,* 1983, Vol. 207, pp. 321-324

[12] Z. Greenwald, et al., "Bunch Length Measurement Using Beam Spectrum", *Conference Record of the 1991 Particle Accelerator Conference,* Vol. 2, pp. 1246-1248, San Francisco, CA, May 1991

[13] A. Temnykh, "Wake function study using two spaced bunches", *Cornell LNS Report CBN 95-11* (1995)

[14] Y. H. Chin, "Advances and Applications of ABCI", *Proceedings of the 1993 Particle Accelerator Conference,* Vol. 2, pp. 3414-3416, Washington, D.C., May 1993

[15] J. DeFord, et al., "The AMOS (Azimuthal Mode Simulator) Code", *Proceedings of the 1989 IEEE Particle Accelerator Conference,* Vol. 2, pp. 1181-1183, Chicago, IL, March 1989
[16] M. Billing, "Higher Mode Power Loss Limitations for Beam Currents in CESR", *Cornell LNS Report CBN 84-15* (1984)
[17] M. Billing, et al., "Measurements of Vacuum Chamber Impedance Effects on the Stored Beam at CESR", *presented at the 1995 Particle Accelerator Conference, Dallas, TX* (to be published)
[18] U. Laustroer, et al., "URMEL and URMEL-T User Guide (Modal Analysis of Cylindrically Symmetric Cavities; Evaluation of RF-Fields in Waveguides)", *DESY M-87-03* (1987)
[19] D. G. Myakishev, V. P. Yakovlev, "The New Possibilities of SuperLANS Code for Evaluation of Axisymmetric Cavities", *presented at the 1995 Particle Accelerator Conference, Dallas, TX* (to be published)
[20] B. Vakoc, "HOM Spectra and Dissipated Power Density Profiles for the SRF cavity with a Ferrite HOM Load: Calculations with CLANS and Analysis", *Cornell LNS Report SRF 950811-11* (1985)
[21] V. Veshcherevich, et al., "Higher Order Modes Damping in CESR B Cavity", *Proceedings of B Factories: The State of the Art in Accelerators, Detectors and Physics,* SLAC-400/CONF-9204126, pp. 177-180, Stanford, CA, April 1992